Atmos. Chem. Phys., 22, 10061–10076, 2022
https://doi.org/10.5194/acp-22-10061-2022


Atmospheric Chemistry and Physics
Open Access
EGU



# Sulfuric acid in the Amazon basin: measurements and evaluation of existing sulfuric acid proxies

**Deanna C. Myers[1], Saewung Kim[2], Steven Sjostedt[3], Alex B. Guenther[2], Roger Seco[4], Oscar Vega Bustillos[5], Julio Tota[6], Rodrigo A. F. Souza[7], and James N. Smith[1]**

[1]Department of Chemistry, University of California, Irvine, CA, USA
[2]Department of Earth System Science, University of California, Irvine, CA, USA
[3]Department of Chemistry, Morgan Community College, Fort Morgan, CO, USA
[4]Institute of Environmental Assessment and Water Research (IDAEA-CSIC), Barcelona, Catalonia, Spain
[5]Instituto de Pesquisas Energéticas e Nucleares, Cidade Universitaria, São Paulo, Brazil
[6]Instituto de Engenharia e Geociencias, Universidade Federal do Oeste do Pará, Santarém, Brazil
[7]Escola Superior de Tecnologia, Universidade do Estado do Amazonas, Manaus, Brazil

**Correspondence:** James N. Smith (jimsmith@uci.edu)

Received: 2 March 2022 – Discussion started: 11 March 2022
Revised: 30 June 2022 – Accepted: 4 July 2022 – Published: 5 August 2022

**Abstract.** Sulfuric acid is a key contributor to new particle formation, though measurements of its gaseous concentrations are difficult to make. Several parameterizations to estimate sulfuric acid exist, all of which were constructed using measurements from the Northern Hemisphere. In this work, we report the first measurements of sulfuric acid from the Amazon basin. These measurements are consistent with concentrations measured in Hyytiälä, Finland, though, unlike Hyytiälä, there is no clear correlation of sulfuric acid with global radiation. There was a minimal difference in sulfuric acid observed between the wet and dry seasons in the Amazon basin. We also test the efficacy of existing proxies to estimate sulfuric acid in this region. Our results suggest that nighttime sulfuric acid production is due to both a stabilized Criegee intermediate pathway and oxidation of $SO_2$ by OH, the latter of which is not currently accounted for in existing proxies. These results also illustrate the drawbacks of the common substitution of radiation for OH concentrations. None of the tested proxies effectively estimate sulfuric acid measurements at night. For estimates at all times of day, a recently published proxy based on data from the boreal forest should be used. If only daytime estimates are needed, several recent proxies that do not include the Criegee pathway are sufficient. More investigation of nighttime sulfuric acid production pathways is necessary to close the gap between measurements and estimates with existing proxies.

## 1 Introduction

Numerous studies have shown that sulfuric acid ($H_2SO_4$) contributes significantly to atmospheric particle concentrations. It has been found to be a key component in the formation of new atmospheric aerosol particles (Almeida et al., 2013; Jen et al., 2016; Fiedler et al., 2005; Korhonen et al., 1999; Kuang et al., 2010; Kulmala et al., 2012, 2004; McMurry et al., 2000; Myllys et al., 2019; Weber et al., 1996, 1997; Yao et al., 2018) and a significant contributor to the growth of new particles (Bzdek et al., 2012; Paasonen et al., 2010; Riipinen et al., 2007; Stolzenburg et al., 2005, 2020; Wehner et al., 2005). New particle formation (NPF) is a major contributor to global cloud condensation nuclei populations (Gordon et al., 2017; Kerminen et al., 2012; Spracklen et al., 2008, 2010). Given its importance in atmospheric particle formation and growth, accurate measurements of atmospheric $H_2SO_4$ concentrations are necessary for understanding atmospheric chemical and thermal processes and accurately simulating new particle formation (Dunne et al., 2016). However, this has been difficult to achieve because of low ambient concentrations ($10^6$–

$10^7$ molec. $cm^{-3}$ or lower), which can only be measured using specialized instrumentation such as a chemical ionization mass spectrometer (CIMS; Dada et al., 2020; Eisele and Bradshaw, 1993; Jokinen et al., 2012; Mikkonen et al., 2011), and because of challenges in deploying and operating these instruments.

Due to these challenges, several studies have developed parameterizations to serve as proxies for $H_2SO_4$ concentrations using its atmospheric sources and sinks (Lu et al., 2019; Weber et al., 1997; Mikkonen et al., 2011; Petäjä et al., 2009). Using measurements of the hydroxyl radical (OH) and sulfur dioxide ($SO_2$), Weber et al. (1997) estimated the daytime concentration of $H_2SO_4$ with known rates of photochemical production and loss by condensation onto existing particle surface area (condensation sink, CS) and showed good agreement with measurements of $H_2SO_4$ concentrations made in Hawaii and Colorado, USA. However, like $H_2SO_4$, OH is difficult to measure due to low concentrations and a relatively short atmospheric lifetime (Eisele and Bradshaw, 1993). Since OH is formed via ozone ($O_3$) photolysis by ultraviolet radiation, and OH concentration has been found to correlate well with UV radiation (Rohrer and Berresheim, 2006), radiation has replaced OH concentrations in current $H_2SO_4$ proxies. This correlation was confirmed by Petäjä et al. (2009), who estimated concentrations of $H_2SO_4$ in Hyytiälä, Finland, using proxies with OH measurements and UV and global radiation as proxies for OH concentration, and found good agreement between estimated and measured $H_2SO_4$ concentrations using both UV and global radiation as OH substitutes. Because global radiation is more frequently measured than UV radiation, Mikkonen et al. (2011) used global radiation to develop proxies based on CIMS measurements of $H_2SO_4$ made in varying environments throughout North America and Europe. They found that the best approximation for all locations depended mainly on radiation strength, with reduced source dependence on the concentration of $SO_2$ and minimal loss contribution from CS. Mikkonen et al. (2011) attributed the reduced dependence on $SO_2$ and CS to these species representing particulate pollution, which would act as both $H_2SO_4$ and OH sinks. Similarly, a proxy developed using measurements of $SO_2$ concentration, UV radiation, and CS from Beijing, China, found that CS plays a relatively minor role in determining concentrations of $H_2SO_4$, except when CS is large (Lu et al., 2019). A high correlation between CS and $SO_2$ concentrations was observed, which Lu et al. (2019), like Mikkonen et al. (2011), attributed to both parameters representing atmospheric pollution. Together, the Mikkonen et al. (2011) and Lu et al. (2019) results demonstrate that using only photochemical production and CS as the source and sink, respectively, of $H_2SO_4$ is insufficient to accurately estimate its concentration across a wide range of locations.

More recent work has considered additional sources and sinks for atmospheric $H_2SO_4$ to improve these estimates. In addition to formation by OH oxidation of $SO_2$, several proxies described in Dada et al. (2020) consider the formation of $H_2SO_4$ from $O_3$ oxidation of biogenic alkenes via stabilized Criegee intermediates (sCI; Mauldin et al., 2012). This production pathway is hypothesized to dominate at nighttime, when OH is a less important oxidant (Mauldin et al., 1998). The loss term in these new Dada et al. (2020) proxies include both the condensation sink and the clustering of $H_2SO_4$ monomers to form new atmospheric particles. Through testing for a variety of environments, Dada et al. (2020) developed $H_2SO_4$ parameterizations representing sites with conditions similar to those used to develop and verify these proxies. They suggest comparison of any site's $H_2SO_4$, OH, $SO_2$, $O_3$, and dominant alkene concentrations, as well as global radiation and CS, to those of the sites studied and use the proxy developed for the environment most similar to that of interest. The Dada et al. (2020) proxies showed good agreement between the measured and estimated concentrations of $H_2SO_4$ for data from sites used in the proxy construction, but thus far, the proxies have been tested on one new environment. Further validation of these proxies is needed by testing them on measurements from a variety of sites.

Though several of the proxies described earlier considered measurements made in varying environments to develop a robust, generalized $H_2SO_4$ proxy (Dada et al., 2020; Mikkonen et al., 2011), only measurements made in the Northern Hemisphere have been used in their construction. Measurements from the Southern Hemisphere need to be considered in order to develop a proxy that accurately estimates $H_2SO_4$ concentrations globally. The Amazon basin has been the focus of recent field work, specifically the Observations and Modeling of the Green Ocean Amazon (GoAmazon2014/5) experiment (Martin et al., 2016), in large part because the biological emissions from the forest contribute significantly to climate and atmospheric composition in South America (Artaxo et al., 2013; Pöschl et al., 2010). This region is characterized by a mixture of pristine biogenic conditions with pollution from Manaus and human activity in the area (Nobre et al., 2016). Natural emissions dominate the wet season (December–May), during which time the wet deposition of accumulation mode particles (diameter between 0.1–2.5 µm) and coarse mode particles (diameter greater than 2.5 µm) reduces concentrations of particles in these size ranges compared to the dry season (August–November). However, recent work has shown that anthropogenic pollutants influence atmospheric particles during the wet season as well (Glicker et al., 2019). Previous measurements in the Amazon basin have reported concentrations of $SO_2$ that were more than an order of magnitude smaller than those measured in remote sites in the Northern Hemisphere (Andreae and Andreae, 1988; Andreae et al., 1990; Martin et al., 2010). From these measurements, model results have suggested that $H_2SO_4$ levels are too low to result in surface-level particle formation (Spracklen et al., 2006). However, measurements of $H_2SO_4$ levels in the Amazon basin have not yet been reported.

This work reports the first measurements of $H_2SO_4$ in the Amazon basin performed using chemical ionization mass spectrometry. The focus of this work is during two intensive operating periods (IOPs) during the GoAmazon2014/5 campaign, with one during the wet season (IOP 1, 9 February–8 March 2014) and one during the dry season (IOP 2, 28 August–5 September 2014). We then assess the efficacy of existing proxy parameterization in estimating $H_2SO_4$ concentrations in the Amazon basin, which is the first location in the Southern Hemisphere to be tested.

## 2 Methods

### 2.1 Site description

All chemical and meteorological measurements were performed during the GoAmazon2014/5 campaign at the T3 site (3.2133° S, 60.5987° W), 10 km northeast of Manacapuru, Brazil (Martin et al., 2016). This site is located in pastureland 70 km west of Manaus, Brazil, in central Amazonia. Measurement facilities deployed to T3 included the Atmospheric Radiation Measurement (ARM) Mobile Facility number 1 (AMF-1), the ARM Mobile Aerosol Observing System (MAOS), and laboratories contained in four modified shipping containers with instruments operated by several research organizations. Air masses arriving at this site typically originate near the coast of the Atlantic Ocean and contain biogenic species from the forest as they travel to the site, with some influence from Manaus. All times are reported in Coordinated Universal Time (UTC).

### 2.2 Instrumentation

#### 2.2.1 Trace gas analysis

Gas-phase concentration measurements of $H_2SO_4$ and OH were made using a selected ion chemical ionization mass spectrometer (SICIMS), the details of which have been reported previously in Jeong et al. (2022), Tanner et al. (1997), and Mauldin et al. (1998). Concentrations of $SO_2$ were measured using a Thermo Fisher Scientific model 43i trace-level-enhanced pulsed fluorescence $SO_2$ analyzer with a detection limit of $7.4 \times 10^9$ molec. cm$^{-3}$. More specific information regarding the operation and calibration of the $SO_2$ analyzer can be found in Springston (2016). A Thermo Fisher Scientific Ozone Analyzer model 49i was used to measure concentrations of $O_3$, based on their absorption of ultraviolet (254 nm) light. More details regarding the operation of this instrument can be found in Springston (2020). Measurements of monoterpene (MT) and isoprene concentrations were obtained using a selected reagent ion proton transfer reaction time-of-flight mass spectrometer (SRI-PTR-TOFMS). These data were calibrated using the ion signal of $C_{10}H_{17}^+$ for $\alpha$-pinene and $C_5H_9^+$ for isoprene and $\alpha$-pinene and isoprene standards. More specific details about the operation of this instrument are reported in Sarkar et al. (2020). All trace gas concentrations are reported as 5 min averages with units of molecules per cubic centimeter (molec. cm$^{-3}$).

#### 2.2.2 Particle number size distribution

Particle number size distributions for particles with electrical mobility diameters 10–496 nm from 00:00 UTC on 5 February to 18:46 UTC on 16 February, and 11–460 nm for the rest of IOP 1 and IOP 2 were collected using a TSI model 3963 scanning mobility particle sizer with a TSI model 3772 condensation particle counter (CPC; ARM, 2014c). Sampled particles were dried to a maximum of 20 % RH before classification (Kuang, 2016). CS was estimated from the number size distributions for particles with mobility diameters 11–460 nm, using the method described in Kulmala et al. (2001, 2012).

#### 2.2.3 Meteorology

Global radiation was measured at the AMF-1 using a precision spectral pyranometer (Eppley; ARM, 2014b). Data were collected in 60 s intervals. Ambient temperature, relative humidity, wind direction, and wind speed were measured at AMF-1 in 60 s intervals (ARM, 2014a). All meteorological data are reported as 5 min averages. HYSPLIT (Hybrid Single-Particle Lagrangian Integrated Trajectory) air mass back-trajectories were calculated every 6 h for each day of the measurement period evaluate influence at the site from the upwind city of Manaus (Rolph et al., 2017; Stein et al., 2015).

### 2.3 Proxies tested

We used measurements of $SO_2$ and OH along with estimates of CS to evaluate the efficacy of the simplest $H_2SO_4$ proxy developed, which includes the photochemical production of $H_2SO_4$ and loss to particle surface area in estimating the concentration of $H_2SO_4$, using the following equation:

$$\frac{\mathrm{d}[H_2SO_4]}{\mathrm{d}t} = k[OH][SO_2] - [H_2SO_4]CS, \quad (1)$$

where $k$ is the temperature-dependent rate constant (DeMore et al., 1997; Sander et al., 2003). Assuming that $H_2SO_4$ production and loss are in a steady state, Eq. (1) can be rearranged to directly calculate the concentration of $H_2SO_4$ (proxy 1; Table 1). To evaluate whether global radiation (GlobRad) is an effective replacement for OH concentrations in the Amazon basin, we used proxy 2, where $k'$ replaces the temperature-dependent rate constant $k$ and is the fitting parameter between the proxy terms and measured concentration of $H_2SO_4$, similar to the proxy reported by Petäjä et al. (2009, Table 1). We also used several of the proxies developed from data sets collected at a variety of locations to assess how well they estimate $H_2SO_4$ concentrations in the Amazon basin. This includes the proxy, which Mikkonen

**Table 1.** Proxies used in this study to estimate sulfuric acid concentrations. Parameter terms are defined in Sect. 2.3.

| Proxy | Equation |
|---|---|
| 1 | $[H_2SO_4] = \frac{k[OH][SO_2]}{CS}$ |
| 2 | $[H_2SO_4] = \frac{k' \cdot \text{GlobRad}[SO_2]}{CS}$ |
| 3 | $[H_2SO_4] = 8.21 \times 10^{-3} \cdot k \cdot \text{GlobRad}[SO_2]^{0.62} \cdot (CS \cdot RH)^{-0.13}$ |
| 4 | $[H_2SO_4] = \frac{CS}{2{\cdot}4.2{\times}10^{-9}} + \left[\left(\frac{CS}{2{\cdot}4.2{\times}10^{-9}}\right)^2 + \frac{[SO_2]}{4.2{\times}10^{-9}}(8.6 \times 10^{-9} \cdot \text{GlobRad} + 6.1 \times 10^{-29}[O_3][\text{Alkene}])\right]^{1/2}$ |
| 5 | $[H_2SO_4] = \frac{CS}{2{\cdot}2.0{\times}10^{-9}} + \left[\left(\frac{CS}{2{\cdot}2.0{\times}10^{-9}}\right)^2 + \frac{[SO_2]}{2.0{\times}10^{-9}}\left(9.0 \times 10^{-9} \cdot \text{GlobRad}\right)\right]^{1/2}$ |

et al. (2011) reported, that best predicted $H_2SO_4$ concentrations across all of the locations they tested, where $k$ is the temperature-dependent rate constant for the reaction of OH with $SO_2$ (DeMore et al., 1997) multiplied by $10^{12}$ (proxy 3; Table 1). Recent proxies developed by Dada et al. (2020) that additionally consider $H_2SO_4$ production via the sCI pathway and loss due to clustering were tested to evaluate the relative importance of these pathways in determining $H_2SO_4$ concentrations in the Amazon basin. Based on the values of the characteristic predictor variables ($[H_2SO_4]$, $[SO_2]$, CS, GlobRad, $[O_3]$, and [Alkene]) detailed in Fig. 9 of that work, we tested proxies representing environments similar to the boreal forest (Hyytiälä, Finland; proxy 4), and representing environments similar to the rural location (Agia Marina, Cyprus) used to develop this proxy (proxy 5). Notably, proxy 4 is the only proxy tested that includes the sCI production pathway, making it possible to assess nighttime $H_2SO_4$ estimations. One of the limitations of the proxies is that they only consider photochemical $H_2SO_4$ production. The equations corresponding to each proxy (numbered 1–5) are shown below in Table 1.

## 3 Results and discussion

Table 2 lists the key variables for the proxies used in this study across both IOPs. Due to instrument malfunctions and challenges associated with operating this instrument in this remote location, only a select number of days from each IOP are included for analysis. The measurements reported here span 14 d across IOP 1 (9–19 February and 5–8 March 2014) and 9 d across IOP 2 (28 August–5 September); thus, the campaign data are more representative of measurements made during IOP 1 (61 % of the total data points). Table 3 compares the median values of key parameters from the entire campaign to those reported from other studies, which serves both to provide context for our measurements and to assess the appropriateness of parameterizations that have been developed for different locales. Measurements of $H_2SO_4$ during both IOPs show a small degree of seasonality (IOP 1 median of $7.82 \times 10^5$ molec. cm$^{-3}$; IOP 2 median of $2.56 \times 10^5$ molec. cm$^{-3}$), indicating that differences between the wet (IOP 1) and dry (IOP 2) seasons do not influence $H_2SO_4$ to a large degree. The campaign median value ($6.73 \times 10^5$ molec. cm$^{-3}$) is within the range reported for the forested sites of Niwot Ridge and Hyytiälä, which suggests that the forest environment may be similar enough to allow the use of the boreal forest proxy reported in Dada et al. (2020). Measured $H_2SO_4$ is a factor of 3–4 less than those from rural (Agia Marina) and urban (Helsinki, Atlanta, Budapest, and Beijing) environments. In summary, the range of these observations suggests that the general proxy from Mikkonen et al. (2011) (proxy 3) and boreal Dada et al. (2020) proxy (proxy 5) may provide reasonable estimations.

Measurements of $SO_2$ and $O_3$ (Table 2) similarly show minimal differences between the wet and dry seasons. Table 3 compares these observations with those from other relevant studies. Observed $SO_2$ concentrations are higher than those from forested sites, and the campaign average is similar to observations from a rural site (Agia Marina) and a mixed urban/rural site (San Pietro Capofiume, Italy, referred to in the table and hereafter as SPC). The observed levels of $SO_2$ are lower than those from urban sites Helsinki, Budapest, Atlanta, and Beijing. Measurements of $O_3$ concentrations during both IOPs are lower than those reported for all sites used in the Dada et al. (2020) and Mikkonen et al. (2011) studies.

Measurements of CS are consistent with previous observations from other sites with dry season CS ($17.0 \times 10^{-3}$ s$^{-1}$) similar to more polluted sites and wet season CS ($4.81 \times 10^{-3}$ s$^{-1}$) similar to forested and rural sites and one urban site (Helsinki). This difference in CS between the two seasons is mainly driven by a the higher concentration of accumulation mode particles present during IOP 2 (e.g., the average concentration of 50–100 nm particles is 1530 cm$^{-3}$) compared to IOP 1 (average of 300 cm$^{-3}$; Fig. S1 in the Supplement). The lower concentrations of accumulation mode particles during IOP 1 is consistent with the increased wet deposition of particles during the wet season (Andreae et al., 2004; Yamasoe et al., 2000). The CS measurements support the use of the Mikkonen et al. (2011) proxy and the Dada et al. (2020) boreal and rural proxies.

We compared the concentrations of isoprene and monoterpenes to determine the dominant alkene, which was used in the Dada et al. (2020) boreal proxy (proxy 4), per the recommendation in that study. Isoprene was observed to

**Table 2.** Summary of the mean, median, 5th–95th percentiles, and standard deviation (SD) of the relevant trace gases, condensation sink, global radiation, and relative humidity measured in the Amazon basin during this study.

| | | IOP 1 (wet season) | IOP 2 (dry season) | Campaign (combined) |
|---|---|---|---|---|
| $[H_2SO_4]$ | Mean | 9.53 | 3.85 | 7.89 |
| $10^5$ molec. cm$^{-3}$ | Median | 7.82 | 2.59 | 6.73 |
| | 5th–95th percentiles | 5.17–20.4 | 1.05–10.8 | 1.66–18.7 |
| | SD | 5.01 | 3.19 | 5.21 |
| [OH] | Mean | 11.1 | 3.85 | 7.78 |
| $10^5$ molec. cm$^{-3}$ | Median | 9.49 | 2.64 | 6.86 |
| | 5th–95th percentiles | 5.42–21.9 | 0.41–11.0 | 0.63–20.2 |
| | SD | 5.23 | 3.49 | 5.79 |
| $[SO_2]$ | Mean | 0.51 | 0.96 | 0.73 |
| $10^{10}$ molec. cm$^{-3}$ | Median | 0.38 | 0.72 | 0.56 |
| | 5th–95th percentiles | 0.11–3.55 | 0.94–6.08 | 0.22–5.02 |
| | SD | 1.16 | 1.83 | 1.72 |
| CS | Mean | 5.45 | 18.7 | 11.6 |
| $10^{-3}$ s$^{-1}$ | Median | 4.81 | 17.0 | 7.54 |
| | 5th–95th percentiles | 1.21–11.8 | 5.13–38.7 | 1.56–31.7 |
| | SD | 4.77 | 12.1 | 11.1 |
| Radiation | Mean | 614 | 666 | 636 |
| ($> 10$) W m$^{-2}$ | Median | 512 | 646 | 587 |
| | 5th–95th percentiles | 39–1460 | 57–1270 | 43–1370 |
| | SD | 465 | 393 | 437 |
| $[O_3]$ | Mean | 2.22 | 4.43 | 3.14 |
| $10^{11}$ molec. cm$^{-3}$ | Median | 1.86 | 3.66 | 2.21 |
| | 5th–95th percentiles | 0.40–5.09 | 0.36–11.2 | 0.38–9.25 |
| | SD | 1.74 | 3.62 | 2.89 |
| [Isoprene] | Mean | 1.82 | 3.15 | 1.98 |
| $10^{11}$ molec. cm$^{-3}$ | Median | 1.10 | 1.98 | 1.62 |
| | 5th–95th percentiles | 0.68–6.32 | 0.72–10.2 | 0.70–7.18 |
| | SD | 2.16 | 4.01 | 2.77 |
| RH | Mean | 90.5 | 82.5 | 88.5 |
| (%) | Median | 95.3 | 88.6 | 94.2 |
| | 5th–95th percentiles | 66.5–99.6 | 52.9–99.5 | 58.8–99.6 |
| | SD | 10.7 | 16.1 | 12.8 |

have a higher concentration (campaign median of $1.62 \times 10^{10}$ molec. cm$^{-3}$) than monoterpenes (campaign median of $3.33 \times 10^9$ molec. cm$^{-3}$) and was thus used in the Dada et al. (2020) boreal estimation as the alkene concentration. The isoprene concentrations measured during the campaign were about an order of magnitude greater than measured monoterpene levels from Hyytiälä, and significantly lower than alkene concentrations measured in Beijing (Dada et al., 2020), supporting the use of the Dada et al. (2020) boreal proxy. The levels of these key variables (CS, $H_2SO_4$, $SO_2$, $O_3$, and isoprene) in estimating the concentration of $H_2SO_4$ in the Amazon basin show that the generalized Mikkonen et al. (2011) proxy and both the boreal and rural Dada et al. (2020) proxies may be appropriate to use in this location.

Next, we compared the 2 h diurnal cycles of the source terms ($SO_2$, OH, and radiation) in the basic photochemical proxies to assess their correlation with the measured concentrations of $H_2SO_4$ (Fig. 1). There is no apparent diurnal cycle of $H_2SO_4$, and notably, there is not a clear correlation between its concentration and the level of global radiation measured at the site. This is in contrast to the correlation observed between these two parameters at the Northern Hemisphere sites used in the construction of the Mikkonen et al. (2011) and Dada et al. (2020) proxies (data sets from Atlanta, USA, Hyytiälä, Finland, Melpitz, Germany, and Niwot Ridge, USA). During the observation period, nighttime concentrations of $H_2SO_4$ accounted for 36 % of the total measured $H_2SO_4$, suggesting that, while photochemical produc-

**Table 3.** Comparison of the median of the relevant trace gases, condensation sink, global radiation, and relative humidity observed during this campaign to those reported from other studies.

| Location | Manacapuru (this study) | Agia Marina[1] | SPC[2] | Niwot Ridge[2] | Hyytiälä[1,3] | Budapest[1] | Beijing[1,3] | Atlanta[2] | Helsinki[1] |
|---|---|---|---|---|---|---|---|---|---|
| Type | Forest/ rural | Rural | Rural/ urban | Forest | Forest | Urban | Urban | Urban | Urban |
| $[H_2SO_4]$ $10^5$ molec. cm$^{-3}$ | 6.73 | 18.1 | 24.0 | 14.0 | 2.3 | 10.2 | 18.1 | 28.5 | 25.5 |
| $[SO_2]$ $10^{10}$ molec. cm$^{-3}$ | 0.56 | 0.46 | 0.59 | 0.44 | 0.14 | 5.45 | 2.42 | 3.79 | 0.87 |
| CS $10^{-3}$ s$^{-1}$ | 7.54 | 3.63 | 6.33 | 3.90 | 3.01 | 10.92 | 22.7 | 15.1 | 3.13 |
| Radiation (> 10) W m$^{-2}$ | 587 | 272.48 | 376 | 207 | 35.4 | 300.56 | 53.62 | 89 | 270.6 |
| $[O_3]$ $10^{11}$ molec. cm$^{-3}$ | 2.21 | – | 9.30 | 13.8 | 8.87 | – | 9.91 | 7.58 | – |
| [Alkene] $10^{11}$ molec. cm$^{-3}$ | 1.62 | – | – | – | 0.27 | – | 12.1 | – | – |
| RH (%) | 94.2 | – | 67 | 52 | – | – | – | 67 | – |

[1] Dada et al. (2020); [2] Mikkonen et al. (2011). [3] These entries are the average of the two campaigns listed in Table S3 of Dada et al. (2020).

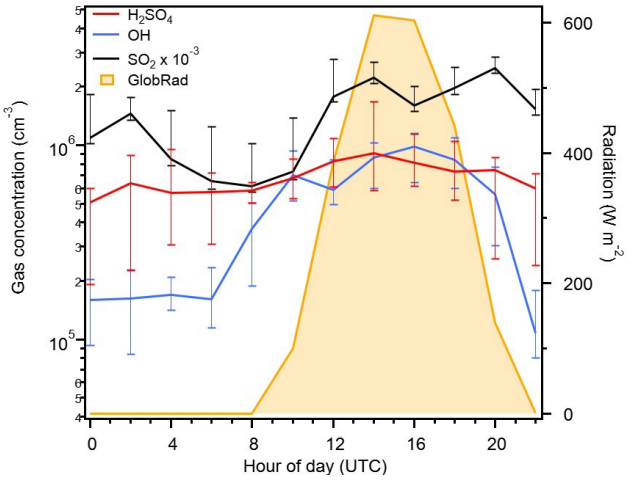


**Figure 1.** The 2 h diurnal variation in the median $H_2SO_4$, $SO_2$, OH, and global radiation measured during the entire campaign. Note that daylight hours are from 08:00–22:00 UTC during the campaign; negligible changes between IOPs 1 and 2 were observed.

tion is likely an important source of $H_2SO_4$ in the Amazon basin, nighttime sources should also be considered in an efficient proxy.

Additionally, Fig. 1 shows that there was OH measured during the nighttime (22:00–08:00 UTC). This suggests that the common use of global radiation as an OH replacement in $H_2SO_4$ proxies is only sufficient during daytime hours (08:00–22:00 UTC) in the Amazon basin. This is consistent with model results from Lelieveld et al. (2008, 2016), which indicate that secondary production of OH through $O_3$ reaction with isoprene is a major source of OH in the boundary layer in the Amazon rainforest, in addition to primary production from photodissociation of $O_3$. This secondary pathway is active at nighttime and likely contributes in other regions where data sets have been used to construct and test $H_2SO_4$ proxies, meaning that nighttime $H_2SO_4$ is not being accounted for in these estimations. Thus, as we move through our testing of the proxies that substitute global radiation for OH, it is with the understanding that this substitution misses the nighttime production of $H_2SO_4$ through the oxidation of $SO_2$ by OH, which is likely occurring in this location. We also note that all of the parameterizations tested include only the oxidation of $SO_2$ to produce $H_2SO_4$, though species such as dimethylsulfide, hydrogen sulfide, and methylmercaptan have been previously measured in the Amazon basin and may contribute to $H_2SO_4$ production (Andreae and Andreae, 1988; Andreae et al., 1990).

Because the measurement site is located downwind of Manaus, the largest city in the state of Amazonia, we used HYSPLIT back trajectories to differentiate between periods with and without influence from Manaus, both of which occurred frequently during IOPs 1 and 2. The 2 h median diurnal variations in $H_2SO_4$, $SO_2$, and OH are shown in Fig. S7. During periods with Manaus influence ($\sim 65\,\%$ of measurements), $SO_2$ measurements tend to be higher but are still within standard deviation of each other, with median values of $0.54 \times 10^{10}$ cm$^{-3}$ (Manaus) and $0.38 \times 10^{10}$ cm$^{-3}$ (no Manaus). Similarly, measured $H_2SO_4$ differed minimally between periods with and without Manaus influence, with median values of $8.77 \times 10^5$ cm$^{-3}$ (Manaus) and $7.40 \times 10^5$ cm$^{-3}$ (no Manaus), though, interestingly, nighttime $H_2SO_4$ is slightly larger when there is minimal influence from Manaus. OH measurements are about twice as large during periods with Manaus influence compared to those without, with median values of $2.40 \times 10^5$ cm$^{-3}$ (Manaus) and $1.24 \times 10^5$ cm$^{-3}$ (no Manaus), and $O_3$ is about 1.5 times larger during periods with Manaus influence, with median values of $3.90 \times 10^5$ cm$^{-3}$ (Manaus) and $2.78 \times 10^{11}$ cm$^{-3}$ (no Manaus). The $O_3$ measurements are consistent with those reported in Kuhn et al. (2010), in which aircraft measurements reported heightened levels of $O_3$ in air masses with Manaus emissions compared to those without. Given the frequency of Manaus influence during both IOPs, the analysis of

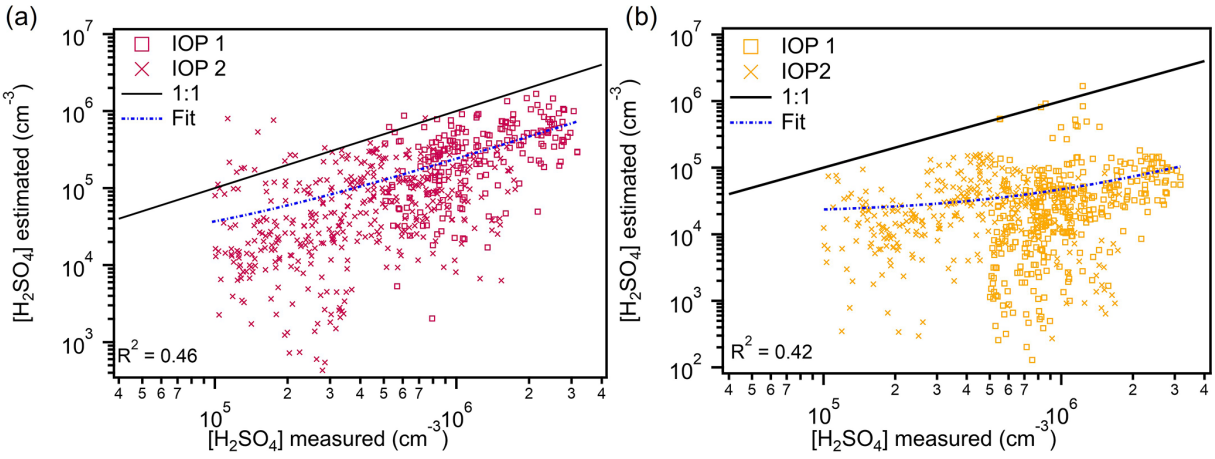


**Figure 2.** Estimated concentrations of sulfuric acid from proxy 1 (865 points) **(a)** and proxy 2 (1941 points) **(b)** versus measured concentrations. Data from IOP 1 are plotted as boxes, and data from IOP 2 are plotted as crosses. The 1 : 1 line is plotted to guide the eye. The fit line represents the fit between the measured and proxy-estimated values of sulfuric acid.

this effect on the $H_2SO_4$ estimations performed in this study is discussed at the end of the results and discussion.

The concentration of $H_2SO_4$ was estimated using proxy 1, which includes production from the oxidation of $SO_2$ by OH and loss from CS. The results of this estimation are plotted as a function of the measured $H_2SO_4$ in Fig. 2a. Estimates from IOPs 1 and 2 fall below the 1 : 1 line, meaning the proxy tends to underestimate measured $H_2SO_4$ by an average factor of 3.7. Despite a generally linear trend exhibited between the estimated and measured values, there is a weak correlation (0.46) between these two that cannot be attributed to a single parameter (CS, OH, and $SO_2$) included in the proxy. While this proxy is advantageous in that it is the only proxy tested that depends directly on the concentrations of species that react to form $H_2SO_4$ and uses measured rate constants to perform estimations, in the Amazon basin this estimation provides a lower limit of $H_2SO_4$ concentrations. Our results further support the hypothesis that there is another source of $H_2SO_4$ in this region that is not described by OH-initiated oxidation of $SO_2$. They also indicate that loss from CS may not be the only loss pathway for $H_2SO_4$.

To evaluate whether global radiation is a sufficient substitute for OH during the daytime, we used proxy 2 to estimate $H_2SO_4$. The value of $k'$ was calculated as a fit parameter between the log of the proxy terms (GlobRad, $SO_2$, and CS) and the log of the measured $H_2SO_4$ for the entire data set (Fig. S2). The calculated value of $k'$ is $2.43 \times 10^{-10}\,m^2\,s^1\,W^{-1}$, which is smaller than the fit value, reported in Petäjä et al. (2009), of $1.4 \times 10^{-7}\,m^2\,s^1\,W^{-1}$. The difference in $k'$ is a result of the dependence of the proxy on radiation between the location used in this study and Hyytiälä, which was used in Petäjä et al. (2009). A drawback to this estimation compared to proxy 1 is that it does not rely on the specific reactants that produce $H_2SO_4$. Figure 2b shows that this estimation, like that from proxy 1, falls below the 1 : 1 line, though to an even larger degree than the first proxy ($R^2 = 0.42$). Interestingly, the fits for both proxy 1 and proxy 2 have slopes of $\sim 40$, highlighting the similar average underestimation of $H_2SO_4$ by both proxies. Measurements of OH and radiation show little correlation during the observation period (Fig. S3), supporting the hypothesis that secondary OH production from $O_3$ reaction with isoprene contributes significantly in this region (Lelieveld et al., 2008, 2016). Similar results are obtained when using the proxy reported by Petäjä et al. (2009, Fig. S4). Both proxies do a particularly poor job of estimating concentrations during IOP 2 (Fig. 2b), in which the estimates do not exhibit a trend with the measured values. This can be attributed to a lack of correlation between $H_2SO_4$ and radiation during this portion of the observation period (Fig. S3a).

Interestingly, the main underestimations made with proxy 2 occur when the value of global radiation falls between 10–100 $W\,m^{-2}$. Previous studies have used 10 $W\,m^{-2}$ (Mikkonen et al., 2011) and 50 $W\,m^{-2}$ (Dada et al., 2020) as the lower cutoff for radiation, although these results indicate that increasing the lower limit for radiation to 100 $W\,m^{-2}$ would likely improve estimates. Since both $H_2SO_4$ and OH were measured when radiation was less than 100 $W\,m^2$ throughout the entire campaign (Fig. S3), this would be at the expense of estimating $H_2SO_4$ during low light (radiation $< 100\,W\,m^{-2}$) conditions, when the secondary production of OH is likely the dominant source of OH. This discrepancy suggests that a combination of other $H_2SO_4$ sources and secondary OH production are contributing to $H_2SO_4$ levels, which is not being accounted for in this parameterization. Further investigation into the relative importance of primary and secondary OH production pathways should be performed to determine a generalized radiation lower cutoff value for application of these general $H_2SO_4$ proxies during daytime hours. Additionally, more examination of the relative con-

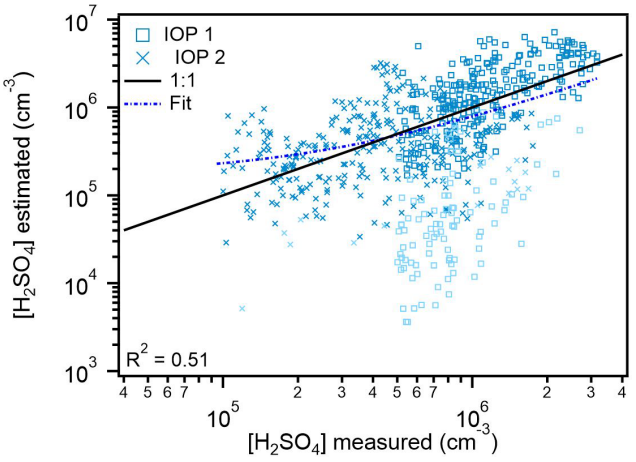


**Figure 3.** Estimated concentrations of sulfuric acid from proxy 3 versus measured concentrations (1172 points). Data from IOP 1 is plotted as boxes, and data from IOP 2 is plotted as crosses. Data points are color-coded to represent the amount of global radiation measured at that time; light blue points were when global radiation was 0–100 W m$^2$, and dark blue points were when global radiation exceeded 100 W m$^2$. The 1 : 1 line is plotted to guide the eye. The fit line represents the fit between the measured and proxy-estimated values of sulfuric acid.

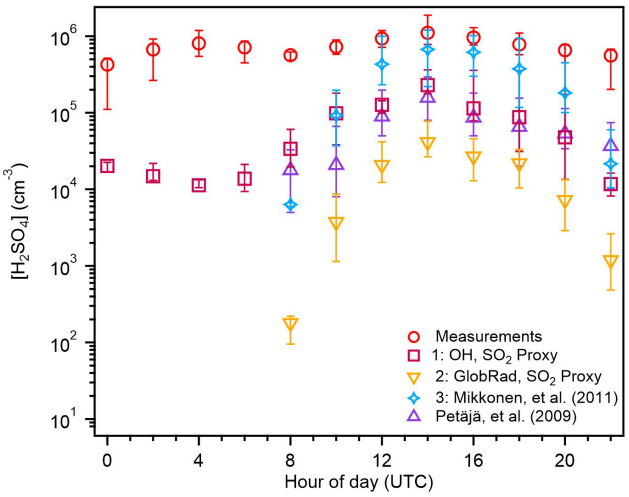


**Figure 4.** The 2 h averaged diurnal variation in the median sulfuric acid measurements (red) and estimations from proxies 1 (purple), 2 (yellow), and 3 (blue) for the entire campaign. The bars represent the 25th–75th percentiles for each measured value. Daylight hours are 08:00–22:00 UTC.

tributions from primary and secondary OH production pathways is necessary to evaluate how well solar radiation represents OH across a range of locations.

The best predictive proxy reported in Mikkonen et al. (2011, proxy 3) was also tested using the Amazon basin data set. Like proxy 2, this uses global radiation instead of OH, though, as described earlier, it was developed using measurements from a variety of different environments and has significant differences in both the $H_2SO_4$ source and sink terms. This proxy has a reduced dependence on $SO_2$ in the source term and a reduced dependence on loss to particle surface area, which includes a term meant to represent particulate hygroscopic growth (CS · RH; Table 1). Figure 3 shows that the estimations from both IOPs fall much closer to the 1 : 1 line than for proxies 1 and 2, with a particularly noticeable improvement for IOP 2 compared to proxy 2. Unlike with proxy 2, the estimations here for IOP 2 exhibit a trend with the measured values of $H_2SO_4$. The lighter-colored markers represent data points where global radiation is between 10–100 W m$^{-2}$. This underestimation during these low light conditions was also seen in the estimates from proxy 2, further supporting the need for the inclusion of secondary OH production in an effective parameterization in the Amazon basin and more investigation into a generalized lower limit for values of radiation used in these parameterizations. These improved estimates from this proxy, with reduced dependence on the concentration of $SO_2$, support the hypothesis reported in Mikkonen et al. (2011) that $SO_2$ is an indicator of particulate pollution, which acts as a sink for both $H_2SO_4$ and OH. Additionally, the Amazon basin is very humid (campaign average RH 89±13 %), and sampled aerosols are dried to below 20 % RH before classification, so accounting for hygroscopic growth of particles in the CS term may better represent the actual particle surface area available for $H_2SO_4$ uptake. This can also help explain the marked improvements over estimates from proxies 1 and 2, both of which underestimate measured $H_2SO_4$.

We plotted the diurnal cycle of each proxy to assess their efficacy in estimating $H_2SO_4$ at different times of the day (Fig. 4). Proxy 1, which is the only proxy to include the concentration of OH, is also the only proxy shown to include nighttime estimations of $H_2SO_4$. Since both species were measured at night in the Amazon basin (Fig. 1), this illustrates a major limitation of the other proxies that use global radiation as a substitute for OH. Despite proxy 1 providing nighttime estimates of $H_2SO_4$, it tends to underpredict measurements by an order of magnitude during these hours. When radiation exceeds 100 W m$^{-2}$ (10:00 UTC; Fig. 1), the proxy reported by Petäjä et al. (2009), which is very similar to proxy 2 in this work, is competitive with proxy 1 in its predictive ability, while proxy 2 is within the 25th percentile of the Petäjä et al. (2009) estimation, and proxy 3 underestimates the measured values by 2 orders of magnitude. From 12:00–20:00 UTC, the Mikkonen et al. (2011) proxy (proxy 3) best estimates the measured concentrations of $H_2SO_4$, and the median estimation falls within the 25th–75th percentiles of the measured values. Proxy 1 and the Petäjä et al. (2009) proxy underestimate measured concentrations by 1 order of magnitude during this time period, while proxy 2 underestimates by $10^1$–$10^2$ molec. cm$^{-3}$. During daylight hours, proxies 1 and 3 are sufficient estimators

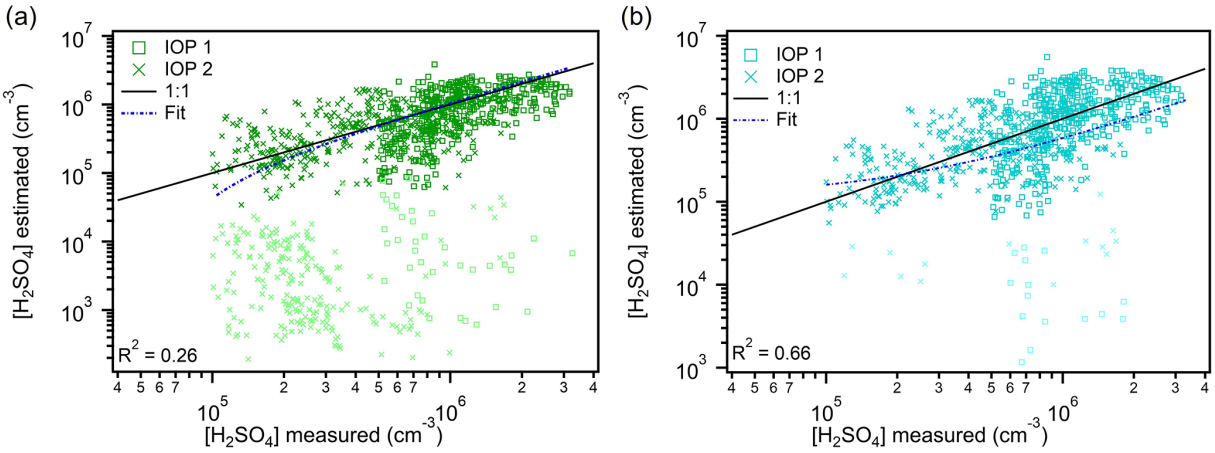


**Figure 5.** Estimated concentrations of sulfuric acid from proxy 4 (1941 points) **(a)** and proxy 5 (1654 points) **(b)** versus measured concentrations. Data from IOP 1 are plotted as boxes, and data from IOP 2 are plotted as crosses. Data points are color-coded to represent the amount of global radiation measured at that time; lighter-colored points were when global radiation was 0–100 W m$^2$, and darker-colored points were when global radiation exceeded 100 W m$^2$. The 1 : 1 line is plotted to guide the eye. The fit line represents the fit between the measured and proxy-estimated values of sulfuric acid.

of $H_2SO_4$, while proxy 2 drastically underestimates measurements. Only proxy 1 can provide nighttime estimations, which are necessary in the Amazon basin, where $H_2SO_4$ is measured at night. This proxy is the only one tested thus far that accounts for secondary OH production.

Several new proxies reported by Dada et al. (2020) include the production of $H_2SO_4$ through a sCI pathway and an additional loss pathway due to clustering of $H_2SO_4$ to form new particles. This additional source of $H_2SO_4$ is active at nighttime, so, despite these proxies depending on global radiation rather than measurements of OH concentration (proxies 4 and 5; Table 1), nighttime estimations can still be made. Based on Fig. 9 of Dada et al. (2020), the proxies developed representing boreal forest and rural environments would be most appropriate to use for the Amazon basin conditions. Of the two proxies, only the boreal (proxy 4) includes the sCI production pathway, though both proxies include the clustering loss term. The rural proxy (proxy 5) can therefore be compared to proxies 1–3 to evaluate the best predictive daytime parameterization for the Amazon basin.

Figure 5a shows that data points where global radiation exceed 100 W m$^{-2}$ from the boreal proxy (proxy 4) fall on the 1 : 1 line, while those from low light conditions all underestimate the measured values. These underestimations ($10^1$–$10^2$ molec. cm$^{-3}$) represent data points from both nighttime and twilight times of day and are likely due to the proxy only considering the sCI formation pathway during these times. The weak correlation (0.26) between the estimated and measured values is driven by the low light data points; a much higher correlation (0.68) is achieved for data points where global radiation $>$ 100 W m$^{-2}$. Since OH was measured during nighttime in the Amazon basin, the production of $H_2SO_4$ from OH oxidation of $SO_2$ is an unaccounted for source in this estimation and likely contributes to the low light underestimations observed. Similar results were obtained using the combined concentrations of isoprene and monoterpene as the alkene term in this proxy (Figs. S5 and S6). Interestingly, the nighttime $H_2SO_4$ production term in this proxy likely also represents the main secondary OH production pathway (Table 1). This illustrates the need to distinguish boreal forest environments from the tropical rainforest due to differences in OH sources; model results suggest that the primary production of OH and secondary production due to $NO_x$ are more important in the boreal forest than tropical rainforest (Lelieveld et al., 2016). The Lelieveld et al. (2016) results also indicate that, even during summertime, nighttime OH is lower in the boreal forest than in the tropical rainforest. As pollution, including $NO_x$, is expected to increase in the Amazon basin, model results made from GoAmazon2014/5 data suggest that OH levels will increase (Liu et al., 2018). Despite the similarity in many of the $H_2SO_4$ key predictor variables between the Amazon basin and Hyytiälä, there are major differences between these two locations that require consideration when using proxy 4.

Proxy 5, which is representative of rural conditions, does not include the sCI pathway and therefore only provides daytime estimations of $H_2SO_4$. Data from both IOPs lie near the 1 : 1 line, though they are more spread out around this line than the daytime estimations from proxy 4 (Fig. 5b). The few low light data points used in this parameterization exhibit the underestimation trend seen in proxies 3 and 4, likely due to a combination of missing the sCI $H_2SO_4$ source and secondary OH production like proxy 3. There is a clear improvement in the predictive strength of this estimation compared to proxy 1, which almost entirely underestimates measured concentrations of $H_2SO_4$ (Fig. 2a).

Both of the Dada et al. (2020) proxies have a higher correlation with measured $H_2SO_4$ when global radiation exceeds 100 W m$^{-2}$ (Fig. 5) than the other radiation-based proxies (Figs. 3 and 4). This suggests that proxies 4 and 5 should have daytime estimations that are more consistent with the Amazon basin measurements than the previous proxies. Additionally, proxy 4 should provide estimates during all hours of the day. Considering the amount of OH measured at nighttime during the campaign, and the underestimation of $H_2SO_4$ during low light hours by proxy 4, we decided to assess the efficacy of proxy 4 if measurements of OH were substituted for global radiation in proxy 4. We also refitted the coefficients of proxy 4 (new proxy shown in Eq. 2), the results of which are shown in Fig. 6.

$$[H_2SO_4] = \frac{CS}{2\cdot\left(3.6\times10^{-8}\right)} + \left[\left(\frac{CS}{2\cdot\left(3.6\times10^{-8}\right)}\right)^2 + \frac{SO_2}{3.6\times10^{-8}}\left(6.4\times10^{-10}\cdot[OH] + 4.5\times10^{-29}[OH][Alkene]\right)\right]^{1/2}. \quad (2)$$

As seen in Fig. 6, substituting measured OH for global radiation in proxy 4 results in estimations that are much closer to the 1 : 1 line. Additionally, it almost entirely eliminates the low light underestimations shown for both IOP 1 and IOP 2 in Fig. 5. There is still a large underestimation mode seen in Fig. 6 for IOP 1, which like that seen in Fig. 5b, corresponds to a period of both low global radiation and low OH. While this underestimation contributes to the lower correlation value ($R^2 = 0.58$), overall there is much better agreement between the new proxy 4 estimates and those made using global radiation, likely because of the better estimates under low light conditions. To test this hypothesis, the diurnal cycles of these proxies and the measurements of $H_2SO_4$ were plotted for comparison.

As hypothesized, the estimations from 12:00–20:00 UTC for proxy 4 and 14:00–20:00 UTC for proxy 5 are within the 25th–75th percentile bars of the $H_2SO_4$ measurements (Fig. 7). Both estimations at 10:00 UTC are similar to those from proxies 1 and 3, and all four estimate more accurately than proxy 2 and the Petäjä et al. (2009) proxy (Fig. 4). The consistency between proxies 3 and 5 during the daylight hours indicates that the clustering of $H_2SO_4$ molecules to form new atmospheric particles is not a major loss source during this time of day. The boreal proxy (proxy 4) greatly underestimates measurements at nighttime ($10^2$ molec. cm$^{-3}$) and are 1 order of magnitude smaller than those from proxy 1 (Fig. 4). In order to match the concentrations of $H_2SO_4$ measured between 00:00–08:00 UTC, there would need to be an increase of $10^3$ molec. cm$^{-3}$ of alkene (median concentration necessary is $2.9\times10^{12}$ molec. cm$^3$), which is larger than the total concentration of monoterpenes and isoprene measured during the campaign (Fig. S6). Substituting OH for global radiation in the boreal proxy, resulting in the parameterization described by Eq. (2), significantly improves these estimates during nighttime hours. However, the underestimation of measurements seen in this proxy at night is likely reflective of the parameterizations not including non-$SO_2$ sources of sulfur. These results suggest that both the sCI and OH oxidation of $SO_2$ are contributors at nighttime in the Amazon basin and perhaps in other locations as well. Estimating $H_2SO_4$ concentrations at night is currently the main area of uncertainty with current proxies, and while

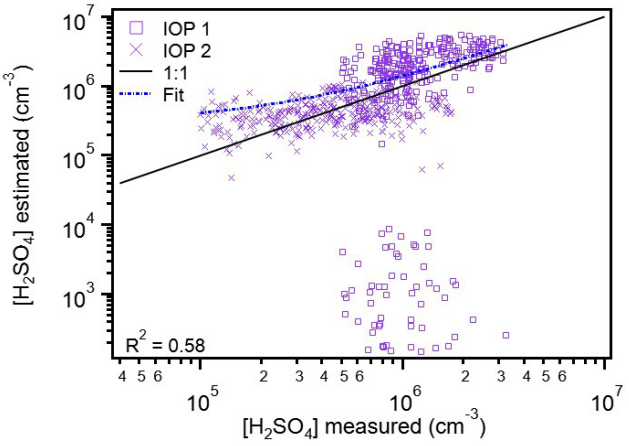


**Figure 6.** Estimated concentrations of sulfuric acid from proxy 4 (8124 points), where measured OH is used instead of global radiation, versus measured concentrations. Data from IOP 1 are plotted as boxes, and data from IOP 2 are plotted as crosses. The proxy coefficients were refitted and are shown in Eq. (2). The 1 : 1 line is plotted to guide the eye. The fit line represents the fit between the measured and proxy-estimated values of sulfuric acid.

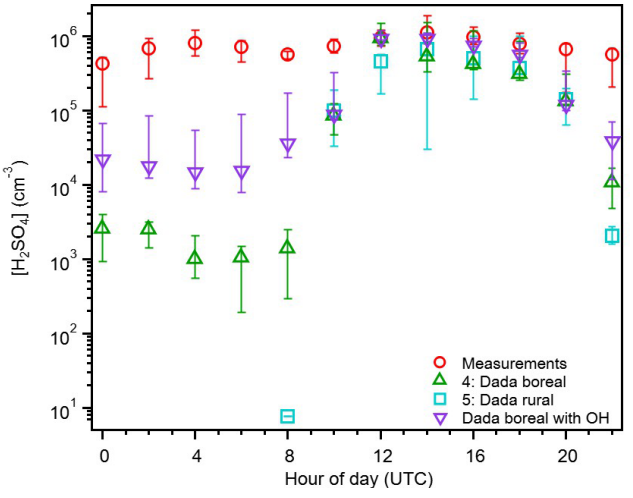


**Figure 7.** The 2 h averaged diurnal variation in the median sulfuric acid measurements (red), and estimations from proxies 4 (green), 5 (teal), and Eq. (2) (purple) for the entire campaign. The bars represent the 25th–75th percentiles for each value. Daylight hours are 08:00–22:00 UTC.

measurements of OH are difficult to make, they are key to determining low light and nighttime sources of $H_2SO_4$ for developing a robust proxy for general use.

The modified boreal proxy from Dada et al. (2020, Eq. 2) is the best general use proxy for the Amazon basin. This proxy provides the most representative estimations of $H_2SO_4$, considering both overall estimations (Fig. 6) and the diurnal cycle compared to measured values (Fig. 7). Though the Mikkonen et al. (2011), boreal, and rural proxies provide similarly accurate estimations during daylight hours, and proxy 4 provides nighttime estimates, substituting OH for global radiation (Eq. 2) provides the most accurate nighttime estimations. Our results support the Dada et al. (2020) recommendation to compare a given location's conditions to those reported in Fig. 9 of that work to determine the most appropriate proxy to use. The conditions in the Amazon basin best aligned with the boreal conditions reported in that work, and of the currently published parameterizations tested, indicate that that proxy provided the best estimates of $H_2SO_4$. We note that caution should be applied to estimates from this parameterization due to differences in OH production pathways between the boreal forest and tropical rainforest environments and recommend substituting OH concentration for global radiation in proxy 4 and refitting the coefficients in that equation when OH measurements are available. These results support the inclusion of the sCI production pathway and loss due to clustering pathway in a robust proxy. They also show that replacing the concentration of OH with global radiation is insufficient for proxies in the Amazon basin, where OH has been measured at nighttime (Fig. 1), and likely contributes to the measured $H_2SO_4$ during this time of day. For estimations of solely daytime concentrations of $H_2SO_4$ (global radiation $> 100\,W\,m^{-2}$), the Dada et al. (2020) estimations (proxies 4 and 5) and Mikkonen et al. (2011) parameterization (proxy 3) provide the best estimations of $H_2SO_4$ (Figs. 3–7). These proxies provide better daytime estimations than the photochemical proxies that only consider production of $H_2SO_4$ via OH oxidation of $SO_2$ and loss solely to particle surface area (CS). As expected by the higher concentrations of OH and $O_3$ measured in periods without Manaus influence, proxies 1 and 4 provided better estimations of $H_2SO_4$ when the site experienced influence from Manaus (Fig. S8). In particular, the nighttime estimating power of these proxies is much improved (by $\sim 10\,cm^{-3}$), suggesting that anthropogenic influence contributes to the nighttime sources of $H_2SO_4$ in this region.

## 4 Conclusions

This paper reports, to the best of our knowledge, the first measurements of $H_2SO_4$ from the Amazon basin. The median concentrations measured during both the wet (IOP 1 is $7.82 \times 10^5$ molec. $cm^{-3}$) and dry (IOP 2 is $2.59 \times 10^5$ molec. $cm^{-3}$) seasons differed only slightly from each other, indicating that seasonal changes have a minimal impact on $H_2SO_4$ in this region. These concentrations are consistent with measured values from the boreal forest in Hyytiälä (Dada et al., 2020; Mikkonen et al., 2011) and are much lower than measurements from more urban locations (Dada et al., 2020; Mikkonen et al., 2011). Our results show minimal diurnal variation across both seasons and no clear correlation with global radiation, which are in contrast previous measurements of $H_2SO_4$ from a variety of locations (Dada et al., 2020; Mikkonen et al., 2011; Petäjä et al., 2009). These results suggest that photochemical oxidation of $SO_2$ by OH is not the only source of $H_2SO_4$ in the region and demonstrate the importance of including measurements from a wide range of sites to develop a general use $H_2SO_4$ proxy.

The best predictive proxy for all light conditions was the boreal proxy reported in Dada et al. (2020), with OH substituted for global radiation, though the published proxy using global radiation was the second best tested here. This was the only radiation-dependent proxy to provide nighttime estimations, which is a clear advantage for use in an environment like this one where there is measurable nighttime $H_2SO_4$. If nighttime estimations of $H_2SO_4$ are necessary for environments similar to the Amazon basin, the boreal proxy reported in Dada et al. (2020) is the best available estimation for low light data when measurements of OH are unavailable. However, we note that the nighttime estimations are incomplete because the production via OH oxidation of $SO_2$ is not included, and including measurements of OH in this parameterization improved nighttime estimates of $H_2SO_4$. Additionally, this parameterization does not include a sink for Criegee intermediates, which may be important in this region with high RH. The validity of the rural proxy from Dada et al. (2020) and the best proxy from Mikkonen et al. (2011) are supported for daytime estimations (radiation $> 100\,W\,m^{-2}$) by these results. All four provide estimations within the 25th to 75th percentile of the measured concentrations under these conditions.

Based on the measurements from the Amazon basin and the proxy results, both the sCI and $SO_2$ oxidation by OH pathways for $H_2SO_4$ production contribute during low light and nighttime conditions. This combination under low light conditions is not currently accounted for by any existing $H_2SO_4$ proxy and may be responsible for low light $H_2SO_4$ in other tropical and low $NO_x$ environments. The combination of biogenic emissions from the rain forest combined with fresh anthropogenic emissions from local farms and aged anthropogenic emissions from Manaus provides more chemical heterogeneity than what is observed in Hyytiälä (Asmi et al., 2011; Dada et al., 2017; Kulmala et al., 2016), which may help explain the observed discrepancy between the measured and estimated $H_2SO_4$ concentrations. More measurements from the Southern Hemisphere, which has lower $NO_x$ compared to the Northern Hemisphere, should be used to test and construct $H_2SO_4$ proxies to more accurately represent the variety of $H_2SO_4$ and OH sources.

These results, which are the first to test existing proxies using data from the Southern Hemisphere, demonstrate the challenges in simplifying the complex processes controlling $H_2SO_4$ levels into an equation. We observed that radiation is not always an effective substitute for OH concentrations, particularly when global radiation is between 0–100 W $m^{-2}$. This substitution is not valid in locations where there is measurable OH at night, due to production from secondary sources such as $O_3$ oxidation of alkenes like isoprene. While OH is difficult to measure, effort should be made to collect more measurements across a variety of environments to assess its contribution to the $H_2SO_4$ population during low light and nighttime conditions and to help develop proxies that more accurately account for this nighttime chemistry. In particular, more OH measurements are needed in the Southern Hemisphere to constrain OH models and improve $H_2SO_4$ parameterizations.

**Data availability.** GoAmazon2014/5 data used in this study are available from the ARM website at https://doi.org/10.5439/1346559 (ARM, 2022).

**Supplement.** The supplement related to this article is available online at: https://doi.org/10.5194/acp-22-10061-2022-supplement.

**Author contributions.** Measurements were made by SK, SS, ABG, RS, OVB, JT, RAFS, and JNS. DM performed proxy estimations, and DM and JNS helped analyze results. DM prepared the paper, with contributions from SK, SS, ABG, RS, OVB, JT, RAFS, and JNS.

**Competing interests.** The contact author has declared that none of the authors has any competing interests.

**Disclaimer.** Publisher's note: Copernicus Publications remains neutral with regard to jurisdictional claims in published maps and institutional affiliations.

**Acknowledgements.** Institutional support for GoAmazon2014/5 was provided by the Central Office of the Large Scale Biosphere Atmosphere Experiment in Amazonia (LBA), the National Institute of Amazonian Research (INPA), and Amazonas State University (UEA) and the local Research Support Foundation (FAPEAM/GOAMAZON). We also acknowledge support from the Atmospheric Radiation Measurement (ARM) Climate Research Facility, a user facility of the United States Department of Energy, Office of Science, sponsored by the Office of Biological and Environmental Research, and support from the Atmospheric System Research (ASR; grant nos. DE-SC0011122 and DE-SC0019000) program of that office. James N. Smith acknowledges support from a Brazilian Science Mobility Program (Programa Ciência sem Fronteiras) Special Visiting Researcher Scholarship. Roger Seco acknowledges grants RYC2020-029216-I and CEX2018-000794-S funded by MCIN/AEI/10.13039/501100011033 and by "ESF Investing in your future". The authors would also like to thank Michelia Dam, Hayley Glicker, Adam Thomas, and Jeremy Wakeen, for their contributions to discussions regarding this project.

**Financial support.** This research has been supported by the Office of Science (grant nos. DE-SC0011122 and DE-SC0019000).

**Review statement.** This paper was edited by Tanja Schuck and reviewed by two anonymous referees.

## References

Almeida, J., Schobesberger, S., Kürten, A., Ortega, I. K., Kupiainen-Määttä, O., Praplan, A. P., Adamov, A., Amorim, A., Bianchi, F., Breitenlechner, M., David, A., Dommen, J., Donahue, N. M., Downard, A., Dunne, E., Duplissy, J., Ehrhart, S., Flagan, R. C., Franchin, A., Guida, R., Hakala, J., Hansel, A., Heinritzi, M., Henschel, H., Jokinen, T., Junninen, H., Kajor, M., Kangasluoma, J., Keskinen, H., Kupc, A., Kurtén, T., Kvashin, A. N., Laaksonen, A., Lehtipalo, K., Leiminger, M., Leppä, J., Louonen, V., Makhmutov, V., Mathot, S., McGrath, M. J., Nieminen, T., Olenius, T., Onnela, A., Petäjä, T., Riccobono, F., Riipinen, I., Rissanen, M., Rondo, L., Ruuskanen, T., Santos, F. D., Sarnela, N., Schallhart, S., Schnitzhofer, R., Seinfeld, J. H., Simon, M., Sipilä, M., Stozhkov, Y., Stratmann, F., Tomé, A., Tröstl, J., Tragkogeorgas, G., Vaatovaara, P., Viisanen, Y., Virtanen, A., Vrtala, A., Wagner, P. E., Weingartner, E., Wex, H., Williamson, C., Wimmer, D., Ye, P., Yli-Juuti, T., Carslaw, K. S., Kulmala, M., Curtius, J., Baltensperger, U., Worsnop, D. R., Vehkamä, H., and Kirkby, J.: Molecular Understanding of Sulphuric Acid–Amine Particle Nucleation in the Atmosphere, Nature, 502, 359–363, https://doi.org/10.1038/nature12663, 2013.

Andreae, M. O. and Andreae, T. W.: The cycle of biogenic sulfur compounds over the Amazon Basin: 1. Dry season, J. Geophys. Res.-Atmos., 93, 1487–1497, https://doi.org/10.1029/JD093ID02P01487, 1988.

Andreae, M. O., Berresheim, H., Bingemer, H., Jacob, D. J., Lewis, B. L., Li, S. M., and Talbot, R. W.: The atmospheric sulfur cycle over the Amazon Basin: 2. Wet season, J. Geophys. Res.-Atmos., 95, 16813–16824, https://doi.org/10.1029/JD095ID10P16813, 1990.

Andreae, M. O., Rosenfeld, D., Artaxo, P., Costa, A. A., Frank, G. P., Longo, K. M., and Silva-Dias, M. A. F.: Smoking Rain Clouds over the Amazon, Science, 303, 1337–1342, https://doi.org/10.1126/science.1092779, 2004.

ARM: Atmospheric Radiation Measurement (ARM) user facility, 2014, updated hourly, Surface Meteorological Instrumentation (MET), 2014-02-09 to 2014-10-01, ARM Mobile Facility (MAO) Manacapuru, Amazonas, Brazil, AMF1 (M1), Compiled by Kyrouac, J. and Holdridge, D., ARM, https://doi.org/10.5439/1025220, 2014a.

ARM: Atmospheric Radiation Measurement (ARM) user facility, 2014, updated hourly, Sky Radiometers on Stand for Downwelling Radiation (SKYRAD60S), 2014-02-09 to 2014-10-01, ARM Mobile Facility (MAO) Manacapuru, Amazonas, Brazil, AMF1 (M1), Compiled by Sengupta, M., ARMhttps://doi.org/10.5439/1025281, 2014b.

ARM: Atmospheric Radiation Measurement (ARM) Climate Research Facility, 2014, updated hourly, Scanning mobility particle sizer (AOSSMPS), 2014-03-13 to 2014-03-24, ARM Mobile Facility (MAO), ARM, https://adc.arm.gov/discovery/#/results/instrument_class_code::smps/site_code::mao/start_date::2014-01-01/end_date::2015-11-30 (last access: 22 October 2021), 2014c.

ARM: Campaign Datasets for Observations and Modeling of the Green Ocean Amazon (GoAmazon), ARM [data set], https://doi.org/10.5439/1346559, 2022.

Artaxo, P., Rizzo, L. V., Brito, J. F., Barbosa, H. M., Arana, A., Sena, E. T., Cirino, G. G., Bastos, W., Martin, S. T., and Andreae, M. O.: Atmospheric aerosols in Amazonia and land use change: From natural biogenic to biomass burning conditions, Faraday Discuss., 165, 203–235, https://doi.org/10.1039/c3fd00052d, 2013.

Asmi, A., Wiedensohler, A., Laj, P., Fjaeraa, A.-M., Sellegri, K., Birmili, W., Weingartner, E., Baltensperger, U., Zdimal, V., Zikova, N., Putaud, J.-P., Marinoni, A., Tunved, P., Hansson, H.-C., Fiebig, M., Kivekás, N., Lihavainen, H., Asmi, E., Ulevicius, V., Aalto, P. P., Swietlicki, E., Kristensson, A., Mihalopoulos, N., Kalivitis, N., Kalapov, I., Kiss, G., de Leeuw, G., Henzing, B., Harrison, R. M., Beddows, D., O'Dowd, C., Jennings, S. G., Flentje, H., Weinhold, K., Meinhardt, F., Ries, L., and Kulmala, M.: Number size distributions and seasonality of submicron particles in Europe 2008–2009, Atmos. Chem. Phys., 11, 5505–5538, https://doi.org/10.5194/acp-11-5505-2011, 2011.

Bzdek, B. R., Zordan, C. A., Pennington, M. R., Luther, G. W., and Johnston, M. V.: Sources and sinks driving sulfuric acid concentrations in contrasting environments: Implications on proxy calculations, Environ. Sci. Technol., 46, 4365–4373, https://doi.org/10.1021/es204556c, 2012.

Dada, L., Paasonen, P., Nieminen, T., Buenrostro Mazon, S., Kontkanen, J., Peräkylä, O., Lehtipalo, K., Hussein, T., Petäjä, P., Kerminen, V.-M., Bäck, J., and Kulmala, M.: Long-term analysis of clear-sky new particle formation events and nonevents in Hyytiälä, Atmos. Chem. Phys., 17, 6227–6241, https://doi.org/10.5194/acp-17-6227-2017, 2017.

Dada, L., Ylivinkka, I., Baalbaki, R., Li, C., Guo, Y., Yan, C., Yao, L., Sarnela, N., Jokinen, T., Daellenbach, K. R., Yin, R., Deng, C., Chu, B., Nieminen, T., Wang, Y., Li, Z., Thakur, R. C., Kontkanen, J., Stolzenburg, D., Sipilä, M., Hussein, T., Paasonen, P., Bianchi, F., Salma, I., T., W., Pikridas, M., Sciare, J., Jiang, J. Liu, Y., Petäjä, P., Kermimen, V.-M., and Kulmala, M.: Sources and sinks driving sulfuric acid concentrations in contrasting environments: Implications on proxy calculations, Atmos. Chem. Phys., 20, 11747–11766, https://doi.org/10.5194/acp-20-11747-2020, 2020.

DeMore, W., Howard, C., Sander, S., Ravishankara, A., Golden, D., Kolb, C., Hampson, R., Molina, M., and Kurylo, M.: Chemical Kinetics and Photochemical Data for Use in Stratospheric Modeling Evaluation Number 12 NASA Panel for Data Evaluation, Jet Propulsion Laboratory, California Institute of Technology, https://jpldataeval.jpl.nasa.gov/pdf/Atmos97_Anotated.pdf (last access: 26 April 2022), 1997.

Dunne, E. M., Gordon, H., Kürten, A., Almeida, J., Duplissy, J., Williamson, C., Ortega, I. K., Pringle, K. J., Adamov, A., Baltensperger, U., Barmet, P., Benduhn, F., Bianchi, F., Breitenlechner, M., Clarke, A., Curtius, J., Dommen, J., Donahue, N. M., Ehrhart, S., Flagan, R. C., Franchin, A., Guida, R., Hakala, J., Hansel, A., Heinritzi, M., Jokinen, T., Kangasluoma, J., Kirkby, J., Kulmala, M., Kupc, A., Lawler, M. J., Lehtipalo, K., Makhmutov, V., Mann, G., Mathot, S., Merikanto, J., Miettinen, P., Nenes, A., Onnela, A., Rap, A., Reddington, C. L., Riccobono, F., Richards, N. A., Rissanen, M. P., Rondo, L., Sarnela, N., Schobesberger, S., Sengupta, K., Simon, M., Sipilä, M., Smith, J. N., Stozkhov, Y., Tomé, A., Tröstl, J., Wagner, P. E., Wimmer, D., Winkler, P. M., Worsnop, D. R., and Carslaw, K. S.: Global atmospheric particle formation from CERN CLOUD measurements, Science, 354, 1119–1124, https://doi.org/10.1126/SCIENCE.AAF2649/SUPPL_FILE, 2016.

Eisele, F. L. and Bradshaw, J. D.: The elusve hydroxyl radical: measuring OH in the atmosphere, Anal. Chem., 65, 927–939, https://doi.org/10.1021/ac00069a723, 1993.

Fiedler, V., Dal Maso, M., Boy, M., Aufmhoff, H., Hoffmann, J., Schuck, T., Birmili, W., Hanke, M., Uecker, J., Arnold, F., and Kulmala, M.: The contribution of sulphuric acid to atmospheric particle formation and growth: A comparison between boundary layers in Northern and Central Europe, Atmos. Chem. Phys., 5, 1773–1785, https://doi.org/10.5194/acp-5-1773-2005, 2005.

Glicker, H. S., Lawler, M. J., Ortega, J., De Sá, S. S., Martin, S. T., Artaxo, P., Vega Bustillos, O., De Souza, R., Tota, J., Carlton, A., and Smith, J. N.: Chemical composition of ultrafine aerosol particles in central Amazonia during the wet season, Atmos. Chem. Phys., 19, 13053–13066, https://doi.org/10.5194/acp-19-13053-2019, 2019.

Gordon, H., Kirkby, J., Baltensperger, U., Bianchi, F., Breitenlechner, M., Curtius, J., Dias, A., Dommen, J., Donahue, N. M., Dunne, E. M., Duplissy, J., Ehrhart, S., Flagan, R. C., Frege, C., Fuchs, C., Hansel, A., Hoyle, C. R., Kulmala, M., Kürten, A., Lehtipalo, K., Makhmutov, V., Molteni, U., Rissanen, M. P., Stozkhov, Y., Tröstl, J., Tsagkogeorgas, G., Wagner, R., Williamson, C., Wimmer, D., Winkler, P. M., Yan, C., and Carslaw, K. S.: Causes and importance of new particle formation in the present-day and preindustrial atmospheres, J. Geophys. Res.-Atmos., 122, 8739–8760, https://doi.org/10.1002/2017JD026844, 2017.

Jen, C. N., Bachman, R., Zhao, J., McMurry, P. H., and Hanson, D. R.: Diamine-sulfuric acid reactions are a potent source of new particle formation, Geophys. Res. Lett., 43, 867–873, https://doi.org/10.1002/2015GL066958, 2016.

Jeong, D., Seco, R., Emmons, L., Schwantes, R., Liu, Y., McKinney, K. A., Martin, S. T., Keutsch, F. N., Gu, D., Guenther, A. B., Vega, O., Tota, J., Souza, R. A. F., Springston, S. R., Watson, T. B., and Kim, S.: Reconciling Observed and Predicted Tropical Rainforest OH Concentrations, J. Geophys. Res.-Atmos., 127, e2020JD032901, https://doi.org/10.1029/2020JD032901, 2022.

Jokinen, T., Sipilä, M., Junninen, H., Ehn, M., Lönn, G., Hakala, J., Petäjä, T., Mauldin, R. L., Kulmala, M., and Worsnop, D. R.: Atmospheric sulphuric acid and neutral cluster measure-

ments using CI-APi-TOF, Atmos. Chem. Phys., 12, 4117–4125, https://doi.org/10.5194/acp-12-4117-2012, 2012.

Kerminen, V. M., Paramonov, M., Anttila, T., Riipinen, I., Fountoukis, C., Korhonen, H., Asmi, E., Laakso, L., Lihavainen, H., Swietlicki, E., Svenningsson, B., Asmi, A., Pandis, S. N., Kulmala, M., and Petäjä, T.: Cloud condensation nuclei production associated with atmospheric nucleation: A synthesis based on existing literature and new results, Atmos. Chem. Phys., 12, 12037–12059, https://doi.org/10.5194/acp-12-12037-2012, 2012.

Korhonen, P., Kulmala, M., Laaksonen, A., Viisanen, Y., McGraw, R., and Seinfeld, J. H.: Ternary nucleation of $H_2SO_4$, $NH_3$, and $H_2O$ in the atmosphere, J. Geophys. Res.-Atmos., 104, 26349–26353, https://doi.org/10.1029/1999jd900784, 1999.

Kuang, C.: Scanning Mobility Particle Sizer Spectrometer Instrument Handbook, DOE/SC-ARM-TR-179, US Department of Energy, https://www.arm.gov/publications/tech_reports/handbooks/smps_handbook.pdf (last access: 22 October 2021), 2016.

Kuang, C., Riipinen, I., Sihto, S.-L., Kulmala, M., McCormick, A. V., and McMurry, P. H.: An improved criterion for new particle formation in diverse atmospheric environments, Atmos. Chem. Phys., 10, 8469–8480, https://doi.org/10.5194/acp-10-8469-2010, 2010.

Kuhn, U., Ganzeveld, L., Thielmann, A., Dindorf, T., Schebeske, G., Welling, M., Sciare, J., Roberts, G., Meixner, F. X., Kesselmeier, J., Lelieveld, J., Kolle, O., Ciccioli, P., Lloyd, J., Trentmann, J., Artaxo, P., and Andreae, M. O.: Impact of Manaus City on the Amazon Green Ocean atmosphere: Ozone production, precursor sensitivity and aerosol load, Atmos. Chem. Phys., 10, 9251–9282, https://doi.org/10.5194/acp-10-9251-2010, 2010.

Kulmala, M., Dal Maso, M., Mäkelä, J. M., Pirjola, L., Väkevä, M., Aalto, P., Miikkulainen, P., Hämeri, K., and O'Dowd, C. D.: On the formation, growth and composition of nucleation mode particles, Tellus B, 53, 479–490, https://doi.org/10.3402/tellusb.v53i4.16622, 2001.

Kulmala, M., Vehkamäki, H., Petäjä, T., Dal Maso, M., Lauri, A., Kerminen, V. M., Birmili, W., and McMurry, P. H.: Formation and growth rates of ultrafine atmospheric particles: A review of observations, J. Aerosol Sci., 35, 143–176, https://doi.org/10.1016/j.jaerosci.2003.10.003, 2004.

Kulmala, M., Petäjä, T., Nieminen, T., Sipilä, M., Manninen, H. E., Lehtipalo, K., Dal Maso, M., Aalto, P. P., Junninen, H., Paasonen, P., Riipinen, I., Lehtinen, K., Laaksonen, A., and Kerminen, V.-M.: Measurement of the nucleation of atmospheric aerosol particles, Nat. Protocol., 7, 1651–1667, https://doi.org/10.1038/nprot.2012.091, 2012.

Kulmala, M., Hämeri, K., Aalto, P. P., Mäkelä, J. M., Pirjola, L., Nilsson, E. D., Buzorius, G., Rannik, Ü., Dal Maso, M., Seidl, W., Hoffman, T., Janson, R., Hansson, H. C., Viisanen, Y., Laaksonen, A., and O'Dowd, C. D.: Overview of the international project on biogenic aerosol formation in the boreal forest (BIOFOR), Tellus B, 53, 324–343, https://doi.org/10.3402/TELLUSB.V53I4.16601, 2016.

Lelieveld, J., Butler, T. M., Crowley, J. N., Dillon, T. J., Fischer, H., Ganzeveld, L., Harder, H., Lawrence, M. G., Martinez, M., Taraborrelli, D., and Williams, J.: Atmospheric oxidation capacity sustained by a tropical forest, Nature, 452, 737–740, https://doi.org/10.1038/nature06870, 2008.

Lelieveld, J., Gromov, S., Pozzer, A., and Taraborrelli, D.: Global tropospheric hydroxyl distribution, budget and reactivity, Atmos. Chem. Phys, 16, 12477–12493, https://doi.org/10.5194/acp-16-12477-2016, 2016.

Liu, Y., Seco, R., Kim, S., Guenther, A. B., Goldstein, A. H., Keutsch, F. N., Springston, S. R., Watson, T. B., Artaxo, P., Souza, R. A., McKinney, K. A., and Martin, S. T.: Isoprene photo-oxidation products quantify the effect of pollution on hydroxyl radicals over Amazonia, Science Adv., 4, eaar2547, https://doi.org/10.1126/sciadv.aar2547, 2018.

Lu, Y., Yan, C., Fu, Y., Chen, Y., Liu, Y., Yang, G., Wang, Y., Bianchi, F., Chu, B., Zhou, Y., Yin, R., Baalbaki, R., Garmash, O., Deng, C., Wang, W., Liu, Y., Petäjä, P., Kerminen, V.-M., Jiang, J., Kulmala, M., and Wang, L.: A proxy for atmospheric daytime gaseous sulfuric acid concentration in urban Beijing, Atmos. Chem. Phys., 19, 1971–1983, https://doi.org/10.5194/acp-19-1971-2019, 2019.

Martin, S., Andreae, M. O., Artaxo, P., Baumgardner, D., Chen, Q., Goldstein, A. H., Guenther, A., Heald, C. L., Mayol-Bracero, O. L., McMurry, P. H., Pauliquevis, T., Pöschl, U., Prather, K. A., Roberts, G. C., Saleska, S. R., Silva Dias, M. A., Spracklen, D. V., Swietlicki, E., and Trebs, I.: Sources and properties of Amazonian aerosol particles, Rev. Geophys., 48, RG2002, https://doi.org/10.1029/2008RG000280, 2010.

Martin, S. T., Artaxo, P., MacHado, L. A., Manzi, A. O., Souza, R. A., Schumacher, C., Wang, J., Andreae, M. O., Barbosa, H. M., Fan, J., Fishc, G., Goldstein, A., Guenther, A., Jimenez, J., Pöschl, U., Silva Dias, M., Smith, J., and Wendisch, M.: Introduction: Observations and Modeling of the Green Ocean Amazon (GoAmazon2014/5), Atmos. Chem. Phys., 16, 4785–4797, https://doi.org/10.5194/acp-16-4785-2016, 2016.

Mauldin, R. L., Frost, G. J., Chen, G., Tanner, D. J., Prevot, A. S. H., Davis, D. D., and Eisele, F. L.: OH measurements during the First Aerosol Characterization Experiment (ACE 1): Observations and model comparisons, J. Geophys. Res.-Atmos., 103, 16713–16729, https://doi.org/10.1029/98JD00882, 1998.

Mauldin, R. L., Berndt, T., Sipilä, M., Paasonen, P., Petäjä, T., Kim, S., Kurtén, T., Stratmann, F., Kerminen, V. M., and Kulmala, M.: A new atmospherically relevant oxidant of sulphur dioxide, Nature, 488, 193–196, https://doi.org/10.1038/nature11278, 2012.

McMurry, P. H., Woo, K. S., Weber, R., Chen, D. R., and Pui, D. Y.: Size distributions of 3–10 nm atmospheric particles: Implications for nucleation mechanisms, Philos. T. Roy. Soc. A, 358, 2625–2642, https://doi.org/10.1098/rsta.2000.0673, 2000.

Mikkonen, S., Romakkaniemi, S., Smith, J. N., Korhonen, H., Petäjä, T., Plass-Duelmer, C., Boy, M., McMurry, P. H., Lehtinen, K. E., Joutsensaari, J., HAmed, A., Mauldin, R., Birmili, W., Spindler, G., Arnold, F., Kulmala, M., and Laaksonen, A.: A statistical proxy for sulphuric acid concentration, Atmos. Chem. Phys., 11, 11319–11334, https://doi.org/10.5194/acp-11-11319-2011, 2011.

Myllys, N., Chee, S., Olenius, T., Lawler, M., and Smith, J.: Molecular-Level Understanding of Synergistic Effects in Sulfuric Acid-Amine-Ammonia Mixed Clusters, J. Phys. Chem. A, 123, 2420–2425, https://doi.org/10.1021/acs.jpca.9b00909, 2019.

Nobre, C. A., Sampaio, G., Borma, L. S., Castilla-Rubio, J. C., Silva, J. S., and Cardoso, M.: Land-use and climate change risks in the amazon and the need of a novel sustainable devel-

opment paradigm, P. Natl. Acad. Sci. USA, 113, 10759–10768, https://doi.org/10.1073/pnas.1605516113, 2016.

Paasonen, P., Nieminen, T., Asmi, E., Manninen, H. E., Petäjä, T., Plass-Dülmer, C., Flentje, H., Birmili, W., Wiedensohler, A., Hõrrak, U., Metzger, A., Hamed, A., Laaksonen, A., Facchini, M. C., Kerminen, V.-M., and Kulmala, M.: On the roles of sulphuric acid and low-volatility organic vapours in the initial steps of atmospheric new particle formation, Atmos. Chem. Phys., 10, 11223–11242, https://doi.org/10.5194/acp-10-11223-2010, 2010.

Petäjä, T., Mauldin, R. L., Kosciuch, E., McGrath, J., Nieminen, T., Paasonen, P., Boy, M., Adamov, A., Kotiaho, T., and Kulmala, M.: Sulfuric acid and OH concentrations in a boreal forest site, Atmos.Chem. Phys., 9, 7435–7448, https://doi.org/10.5194/acp-9-7435-2009, 2009.

Pöschl, U., Martin, S. T., Sinha, B., Chen, Q., Gunthe, S. S., Huffman, J. A., Borrmann, S., Farmer, D. K., Garland, R. M., Helas, G., Jimenez, J. L., King, S. M., Manzi, A., Mikhailov, E., Pauliquevis, T., Petters, M. D., Prenni, A. J., Roldin, P., Rose, D., Schneider, J., Su, H., Zorn, S. R., Artaxo, P., and Andreae, M. O.: Rainforest aerosols as biogenic nuclei of clouds and precipitation in the Amazon, Science, 329, 1513–1516, https://doi.org/10.1126/science.1191056, 2010.

Riipinen, I., Sihto, S.-L., Kulmala, M., Arnold, F., Dal Maso, M., Birmili, W., Saarnio, K., Teinilä, K., Kerminen, V.-M., Laaksonen, A., and Lehtinen, K.: Connections between atmospheric sulphuric acid and new particle formation during QUEST III–IV campaigns in Heidelberg and Hyytiälä, Atmos. Chem. Phys., 7, 1899–1914, https://doi.org/10.5194/acp-7-1899-2007, 2007.

Rohrer, F. and Berresheim, H.: Strong correlation between levels of tropospheric hydroxyl radicals and solar ultraviolet radiation, Nature, 442, 184–187, https://doi.org/10.1038/nature04924, 2006.

Rolph, G., Stein, A., and Stunder, B.: Real-time Environmental Applications and Display sYstem: READY, Environ. Model. Softw., 95, 210–228, https://doi.org/10.1016/j.envsoft.2017.06.025, 2017.

Sander, S. P., Friedl, R. R., Ravishankara, A. R., Kolb, C. E., Kurylo, M. J., Huie, R. E., Orkin, V. L., Molina, M. J., Moortgat, G. K., and Finlayson-Pitts, B. J.: Chemical Kinetics and Photochemical Data for Use in Atmospheric Studies Evaluation Number 14 NASA Panel for Data Evaluation, NASA, http://jpldataeval.jpl.nasa.gov/ (last access: 16 April 2022), 2003.

Sarkar, C., Guenther, A. B., Park, J. H., Seco, R., Seco, R., Alves, E., Alves, E., Batalha, S., Santana, R., Kim, S., Smith, J., Tóta, J., and Vega, O.: PTR-TOF-MS eddy covariance measurements of isoprene and monoterpene fluxes from an eastern Amazonian rainforest, Atmos. Chem. Phys., 20, 7179–7191, https://doi.org/10.5194/acp-20-7179-2020, 2020.

Spracklen, D. V., Carslaw, K. S., Kulmala, M., Kerminen, V.-M., Mann, G. W., and Sihto, S. L.: The contribution of boundary layer nucleation events to total particle concentrations on regional and global scales, Atmos. Chem. Phys., 6, 5631–5648, https://doi.org/10.5194/acp-6-5631-2006, 2006.

Spracklen, D. V., Carslaw, K. S., Kulmala, M., Kerminen, V. M., Sihto, S. L., Riipinen, I., Merikanto, J., Mann, G. W., Chipperfield, M. P., Wiedensohler, A., Birmili, W., and Lihavainen, H.: aContribution of particle formation to global cloud condensation nuclei concentrations, Geophys. Res. Lett., 35, L06808, https://doi.org/10.1029/2007GL033038, 2008.

Spracklen, D. V., Carslaw, K. S., Merikanto, J., Mann, G. W., Reddington, C. L., Pickering, S., Ogren, J. A., Andrews, E., Baltensperger, U., Weingartner, E., Boy, M., Kulmala, M., Laakso, L., Lihavainen, H., Kivekäs, N., Komppula, M., Mihalopoulos, N., Kouvarakis, G., Jennings, S. G., O'Dowd, C., Birmili, W., Wiedensohler, A., Weller, R., Gras, J., Laj, P., Sellegri, K., Bonn, B., Krejci, R., Laaksonen, A., Hamed, A., Minikin, A., Harrison, R. M., Talbot, R., and Sun, J.: Explaining global surface aerosol number concentrations in terms of primary emissions and particle formation, Atmos. Chem. Phys., 10, 4775–4793, https://doi.org/10.5194/acp-10-4775-2010, 2010.

Springston, S. R.: Sulfur Dioxide Monitor Instrument Handbook, DOE/SC-ARM-TR-180, US Department of Energy, https://www.arm.gov/publications/tech_reports/handbooks/so2_handbook.pdf (last access: 15 April 2022), 2016.

Springston, S. R.: Ozone Monitor (OZONE) Instrument Handbook, DOE/SC-ARM-TR-179, US Department of Energy, https://www.arm.gov/publications/tech_reports/handbooks/ozone_handbook.pdfhttps://www.arm.gov/publications/tech_reports/handbooks/ozone_handbook.pdf (last access: 8 February 2022), 2020.

Stein, A., Draxler, R., Rolph, G., Stunder, B., Cohen, M., and Ngan, F.: NOAA's HYSPLIT Atmospheric Transport and Dispersion Modeling System, B. Am. Meteorol. Soc., 96, 2059–2077, https://doi.org/10.1175/BAMS-D-14-00110.1, 2015.

Stolzenburg, D., Simon, M., Ranjithkumar, A., Kürten, A., Lehtipalo, K., Lehtipalo, K., Gordon, H., Ehrhart, S., Finkenzeller, H., Pichelstorfer, L., Niemenen, T., He, X., Brilke, S., Xiao, M., Amorim, A., Baalbaki, R., Baccarini, A., Beck, L., Bräkling, S., Murillo, L., Chen, D., Chu, B., Dada, L., Dias, A., Dommen, J., Duplissy, J., El Haddad, I., Fischer, L., Carracedo, L., Heinritzi, M., Kim, C., Koenig, T., Kong, W., Lamkaddam, H., Lee, C., Leiminger, M., Li, Z., Makhmutov, V., Manninen, H., Marie, G., Marten, R., Müller, T., Nie, W., Partoll, E., Petäjä, T., Pfeifer, J., Philippov, M., Rissanen, M., Rörup, B., Schobesberger, S., Schuchmann, S., Shen, J., Sipilä, M., Steiner, G., Stozhkov, Y., Tauber, C., Tham., Y., Tomé, A., Vazquez-Pufleau, M., Wagner, A., Wang, M., Wang, Y., Weber, S., Wimmer, D., Wlasits, P., Wu, Y., Ye, Q., Zauner-Wieczorek, M., Baltensperger, U., Carslaw, K., Curtius, J., Donahue, N., Flagan, R., Hansel, A., Kulmala, M., Lelieveld, J., Volkamer, R., Kirkby, J., and Winkler, P.: Enhanced growth rate of atmospheric particles from sulfuric acid, Atmos. Chem. Phys., 20, 7359–7372, https://doi.org/10.5194/acp-20-7359-2020, 2020.

Stolzenburg, M. R., McMurry, P. H., Sakurai, H., Smith, J. N., Mauldin, R. L., Eisele, F. L., and Clement, C. F.: Growth rates of freshly nucleated atmospheric particles in Atlanta, J. Geophys. Res.-Atmos., 110, 1–10, https://doi.org/10.1029/2005JD005935, 2005.

Tanner, D. J., Jefferson, A., and Eisele, F. L.: Selected ion chemical ionization mass spectrometric measurement of OH, J. Geophys. Res.-Atmos., 102, 6415–6425, https://doi.org/10.1029/96jd03919, 1997.

Weber, R. J., Marti, J. J., McMurry, P. H., Eisele, F. L., Tanner, D. J., and Jefferson, A.: Measured atmospheric new particle formation rates: Implications for nu-

cleation mechanisms, Chem. Eng. Commun., 151, 53–64, https://doi.org/10.1080/00986449608936541, 1996.

Weber, R. J., Marti, J. J., McMurry, P. H., Eisele, F. L., Tanner, D. J., and Jefferson, A.: Measurements of new particle formation and ultrafine particle growth rates at a clean continental site, J. Geophys. Res.-Atmos., 102, 4375–4385, https://doi.org/10.1029/96jd03656, 1997.

Wehner, B., Petäjä, T., Boy, M., Engler, C., Birmili, W., Tuch, T., Wiedensohler, A., and Kulmala, M.: The contribution of sulfuric acid and non-volatile compounds on the growth of freshly formed atmospheric aerosols, Geophys. Res. Lett., 32, 1–4, https://doi.org/10.1029/2005GL023827, 2005.

Yamasoe, A., Artaxo, P., Miguel, A. H., and Allen, A. G.: Chemical composition of aerosol particles from direct emissions of vegetation "res" in the Amazon Basin: water-soluble species and trace elements, Atmos. Environ., 34, 1641–1653, 2000.

Yao, L., Garmash, O., Bianchi, F., Zheng, J., Yan, C., Kontkanen, J., Junninen, H., Mazon, S. B., Ehn, M., Paasonen, P., Sipilä, M., Wang, M., Wang, X., Xiao, S., Chen, H., Lu, Y., Zhang, B., Wang, D., Fu, Q., Geng, F., Li, L., Wang, H., Qiao, L., Yang, X., Chen, J., Kerminen, V.-M., Petäjä, T., Worsnop, D., Kulmala, M., and Wang, L.: Atmospheric new particle formation from sulfuric acid and amines in a Chinese megacity, Science, 361, 278–281, https://doi.org/10.1126/science.aao4839, 2018.